



Synthesis and characterization of α,ω -disubstituted quaterthiophenes functionalized with polar groups for solution processed OTFTs

Giuseppe Romanazzi^a, Francesco Marinelli^b, Piero Mastrorilli^a, Luisa Torsi^{b,c}, Ahlam Sibaoui^d, Minna Räisänen^d, Timo Repo^d, Pinalysa Cosma^b, Gian Paolo Suranna^{a,*}, Cosimo Francesco Nobile^a

^a Dipartimento di Ingegneria delle Acque e di Chimica (DIAC), Politecnico di Bari, via Orabona 4, 70125 Bari, Italy

^b Dipartimento di Chimica, Università degli Studi di Bari, 70125 Bari, Italy

^c Centro di Eccellenza TIRES, Università degli Studi di Bari, 70125 Bari, Italy

^d Laboratory of Inorganic Chemistry, Department of Chemistry, University of Helsinki, PO Box 55, 00014 Helsinki, Finland

ARTICLE INFO

Article history:

Received 4 June 2009

Received in revised form 3 September 2009

Accepted 17 September 2009

Available online 19 September 2009

ABSTRACT

A series of soluble quaterthiophenes (**4Ta–g**) bearing ester groups in the α,ω -terminal positions separated from the quaterthiophene core by ethylene (**4Ta–c**), vinylene (**4Td–f**) or ethynylene (**4Tg**) spacers was synthesized by means of a Pd-catalyzed homocoupling of bithiophenes proceeding via C–H bond activation. The synthetic approach gave satisfying yields of **4Ta–f** but resulted in only 3% yield of **4Tg** due to the competitive hydrofluorination of the triple bond. The quaterthiophenes **4Ta–g** were characterized by NMR, FTIR, UV–vis, PL spectroscopies, HRMS, TGA and CV. Thin-films of **4Ta–g** were deposited either by spin-coating or by thermal evaporation on Si/SiO₂ for the fabrication of top-contact OTFTs. The devices prepared using **4Ta–c** bearing the ester functional group separated from the quaterthiophene core by an ethylene spacer showed average hole field-effect mobility up to $2.7 \times 10^{-3} \text{ cm}^2 \text{ V}^{-1} \text{ s}^{-1}$ and up to $6 \times 10^{-3} \text{ cm}^2 \text{ V}^{-1} \text{ s}^{-1}$ for solution processed and for thermally evaporated OTFTs, respectively. The remarkably high solubility of **4Ta–c**, along with their respectable performances in OTFTs render these molecules promising for practical applications as active layers in chemically-sensitive devices.

© 2009 Elsevier Ltd. All rights reserved.

1. Introduction

The research on organic semiconductors to be employed in electronic devices such as organic thin film transistors (OTFTs) benefits from the continuous improvement of the available synthetic tools.¹ In this field, monodispersed α,ω -oligothiophenes have increasingly attracted scientific interest due to their high mobility and on/off ratios exhibited in devices. Since the discovery of the charge transport properties of α -sexithiophene² a continuously increasing interest has been devoted to OTFTs based on both unsubstituted and substituted thiophene oligomers and, in particular, several studies have dealt with the synthesis and characterization of well-defined α,ω -dialkylated quaterthiophenes or sexithiophenes aiming at obtaining more soluble and processable derivatives, while preserving or even improving their electronic properties with respect to α -sexithiophene.³

It is well known that the introduction of functional groups different from alkyl ones onto an oligothiophene core, eventually allows the fine tuning of the electronic and optical properties of the

conjugated backbone.^{3,4} In the perspective of using oligothiophenes as active layers in chemically sensitive OTFTs,^{5,6} the functionalization with polar groups assumes a greater importance, because it can enhance the sensing layer-analyte interactions needed to achieve a high sensing response.

So far, few reports have dealt with the synthesis of oligothiophenes bearing polar side groups and their use in OTFT devices. The field effect transistor mobilities reported range between 10^{-4} and $10^{-2} \text{ cm}^2 \text{ V}^{-1} \text{ s}^{-1}$.⁷

The strategy of introducing different terminal groups to cap the oligothiophene core, however, can be useful for tuning their electronic and optical properties or, in the case of some acetylenic-end substituted oligothiophenes, to obtain liquid crystalline semiconductors.⁸

In this framework, we have recently synthesized and tested the electrical properties of a series of sexithiophenes bearing amide or ester functionalities in the α,ω -positions showing, in the best case, the remarkable mobility of $1.2 \times 10^{-2} \text{ cm}^2 \text{ V}^{-1} \text{ s}^{-1}$.^{7h}

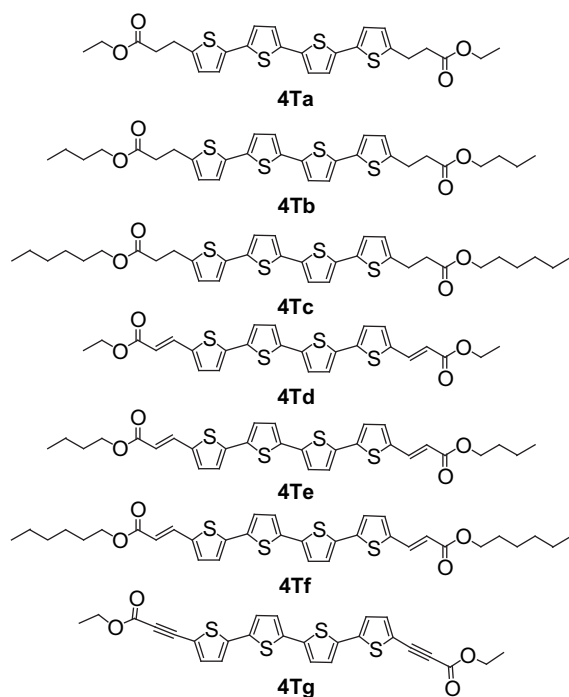
Several synthetic pathways can be applied to the synthesis of oligothiophenes. Among them, the classical oxidative homocoupling of thiophenes mediated by FeCl₃⁹ or CuCl₂¹⁰ suffers from regioselectivity, and the Cu-based procedure even requires a preventive metallation of the thiophene C–H bond with *n*-BuLi,

* Corresponding author. Tel.: +39 080 5963611; fax: +39 080 5963603.

E-mail address: surannag@poliba.it (G.P. Suranna).

a reagent incompatible with the presence of several functional groups. Wider functional group tolerance is granted by the Stille cross-coupling^{11,12}, which, however, produces a significant amount of higher homologues. Recently, Mori et al. have proposed a Pd(II)/AgF catalyzed homocoupling of thiophenes.¹³ This procedure envisages a C–H bond activation and is potentially tolerant towards several functional groups. To date, only few examples of applications of Mori's coupling conditions to the preparation of thiophene-based semiconducting materials have been reported.¹⁴

Intrigued by the comparable mobility exhibited by the α,ω -disubstituted-quaterthiophenes with respect to the corresponding sexithiophenes,¹⁵ we deemed it worthwhile to apply Mori's protocol to obtain soluble α,ω -disubstituted-quaterthiophenes bearing polar groups bound to the oligothiophene core by ethylene, vinylene¹⁶ or ethynylene⁸ spacers (Scheme 1). The higher solubility of shorter thiophene oligomers may allow their deposition as OTFT active layers by wet techniques.¹⁷ Moreover, quaterthiophenes are less sensitive to atmospheric doping, that is, known to decrease the on/off ratio and alter the threshold voltage in OTFTs.^{3d}



Scheme 1.

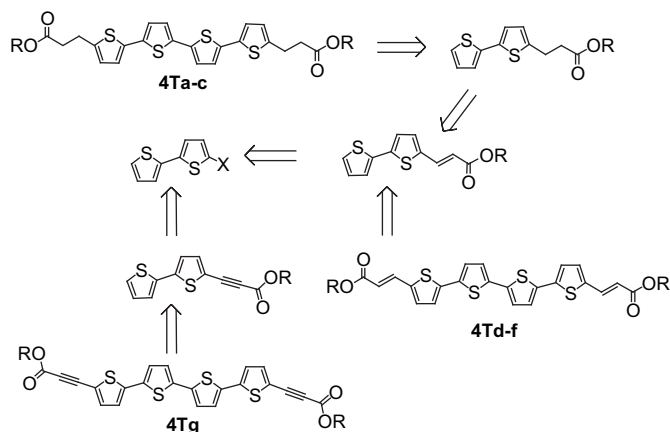
2. Results and discussion

2.1. Synthesis and characterization

The disconnection approach followed for the preparation of the quaterthiophenes, object of this study is shown in Scheme 2.

The monofunctionalized bithiophenes **1–6** (Scheme 3) were subjected to homocoupling using as typical conditions a catalytic amount (3% mol) of PdCl₂(PhCN)₂ in the presence of 2 equiv of AgF in DMSO at 70 °C for one day (Scheme 4).

The oligomers **4Ta–f** were obtained in yields ranging from 51 to 71% as yellow (**4Ta–c**) or red-orange (**4Td–f**) powders. Their solubility in common organic solvents permitted their purification by flash chromatography and their characterization by solution NMR and ESI-MS. For compounds **4Td–f**, the *E*-stereochemistry of their precursors (**1**, **3** and **5**, respectively) was retained as indicated by the values of the $^3J_{\text{H,H}}$ of 15.6 Hz of vinyl protons and by the 980–960 cm^{−1} IR band.



Scheme 2. The retrosynthetic approach followed for the preparation of **4Ta–g**.

The preparation of the oligomer **4Tg**, containing the ethyl ester functionality in direct conjugation with the quaterthiophene core by an ethynylene spacer (Scheme 1) was also addressed. With this aim, the bithiophene derivative **7** (Scheme 3) was prepared in 78% yield by the Pd-catalyzed reaction of 3-zinc ethyl propionate with 5-iodo-2,2'-bithiophene. However, carrying out the homocoupling of **7** under the conditions reported for the preparation of **4Ta–f** (Scheme 5), only a very low amount (3%) of **4Tg** could be isolated, three fluorinated oligothiophenes: **8** (5%, *Z/E*=96/4), **4TgHF** (12%) and **4TgH₂F₂** (26%) being obtained in a consistently higher yield.

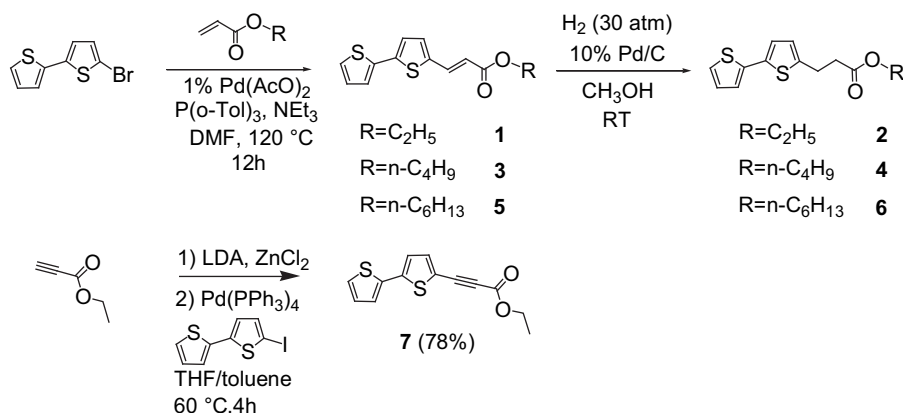
The structures of **4Tg**, **4TgHF** and **4TgH₂F₂** were confirmed by ESI-MS and multinuclear NMR, which showed a remarkably high stereoselectivity towards the *Z* isomer¹⁸ for **4TgHF** and **4TgH₂F₂** as indicated by the value of $^3J_{\text{H,F}}$ =32.7 Hz found for the coupling constant between the vinyl hydrogen and the fluorine.¹⁹

The formation of hydrofluorination byproducts can be explained as the consequence of the HF formation during the catalytic cycle,^{13a} being the addition of HF to the alkynes activated by electron-withdrawing groups a favoured process. The addition of HF can take place directly onto the substrate **7**, yielding the fluorinated product **8**, which in turn may react with **7** yielding **4TgHF** as well as with itself, yielding **4TgH₂F₂**. The latter two compounds can obviously be formed by reaction of **4Tg** or **4TgHF** with HF.

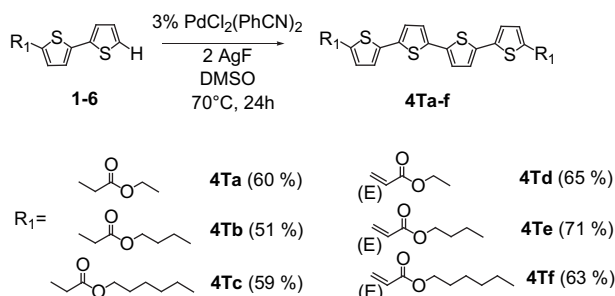
Our findings parallel the *trans*-hydrofluorination observed upon reaction of alkynes activated with highly electron-withdrawing groups with [H₂F₃][−] salts²⁰ or with CsF in wet DMF²¹ where HF is produced in situ. The main difference between metal-free and Pd(II)/AgF systems is the higher stereoselectivity observed in the latter case, pointing out the importance of the fluoride source in order to trigger and sustain the homocoupling reaction, suggesting the intermediacy of a fluoropalladium complex in the catalytic cycle.^{13c}

In order to increase the yield of **4Tg**, the homocoupling of **7** was also carried out in the presence of calcium oxide (from 3 to 10 equiv with respect to **7**) as HF scavenger²² with the result that the formation of the fluorinated oligothiophene **8**, **4TgHF** and **4TgH₂F₂** was completely inhibited and that the yields of **4Tg** was slightly higher (up to 9% after 24 h). A plausible explanation for the diminished activity of the catalytic system in the presence of CaO may reside in the formation of Ag₂O (by reaction of CaO with AgF), which is known to be ineffective in the homocoupling reaction.^{13a}

High resolution ESI-MS spectrograms of **4Ta–g** in CHCl₃/CH₃OH using sodium formate as calibrant, appear as the superimposition of the pattern of the monocationic sodium adduct [**4T**+Na]⁺ with that of the dicationic disodium adduct [(**4T**)₂+2Na]²⁺. Figure 1 shows the representative HRMS spectrogram for **4Tb**, in which the most intense peak (*m/z*=609.1232) corresponds to that calculated



Scheme 3. Synthetic sequence for the preparation of bithienyl precursors 1–7.

Scheme 4. Preparation of the α,ω -quaterthiophenes 4Ta–f.

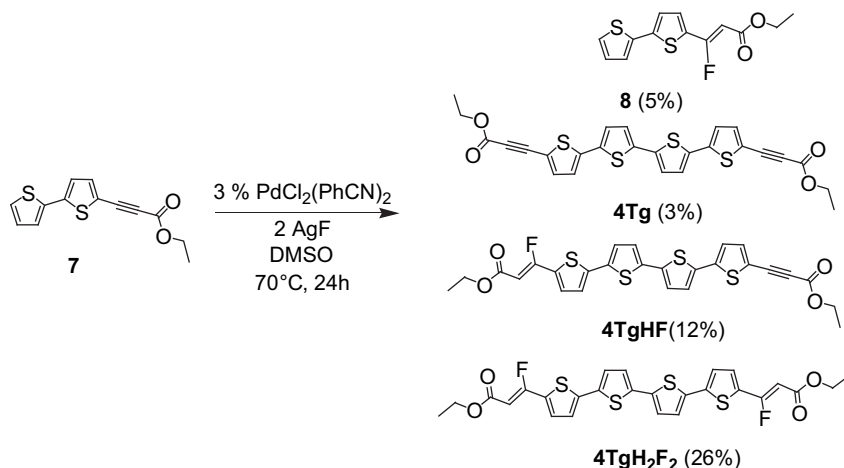
(609.1232) and is due to the all- ^{12}C , all- ^{32}S ($[\text{4Tb}] + \text{Na}$) $^+$ isotopomer, while the one appearing at m/z 610.1257 is attributable to the ($[\text{4Tb}] + \text{Na}$) $^+$ isotopomers containing one ^{13}C atom or one ^{33}S atom. The weak peak appearing between the former two at m/z 609.6262 (calculated: m/z 609.6247) can be clearly attributed to the isotopomers of the doubly charged dimer $[(\text{4Tb})_2 + 2\text{Na}]^{2+}$ containing either only one ^{13}C atom or one ^{33}S atom.²³ A similar behaviour in solution for an α,ω -disubstituted sexithiophene solution was already observed by nanospray Fourier-transform ion cyclotron resonance (FT-ICR) mass spectrometry.²⁴

2.2. Optical and thermal properties

The photophysical properties of the oligothiophenes **4Ta–g** were investigated by UV–vis and photoluminescence (PL) spectroscopies and are summarized in Table 1.

In CHCl_3 solution the optical features of **4Ta–c** are perfectly superimposable, showing a structure less absorption maximum at 400 nm (Fig. 2A), a value nearly equal to those found for related dialkyl quaterthiophenes.²⁵ The spectra of **4Td–f** (Fig. 2B) are also superimposable and show a λ_{max} of 455 nm, which is strongly red shifted with respect to both unsubstituted quaterthiophene ($\lambda_{\text{max}} = 390 \text{ nm}$)²⁶ and dialkyl quaterthiophenes. Figure 2A shows also the emission spectra obtained for **4Ta**. The PL spectrum of **4Ta** in solution shows a structured emission band at 462 nm (λ_{max}) with a vibronic replica at 491 nm and a shoulder at $\sim 522 \text{ nm}$. The splitting of the emission bands is due to vibronic coupling, indicating that, upon photoexcitation, the emitting species adopt a more planar structure with a greater quinoid character. This change in conformation to a more planar structure is manifest in the Stokes shift, whose magnitude (0.42 eV) is estimated as the difference between λ_{abs} and λ_{em} .

The photoluminescence quantum yields (ϕ) for **4Ta–c** were also determined and their values (0.41–0.43) range between those of unsubstituted quaterthiophene and dialkylquaterthiophene.²⁷ The energy gap in solution, evaluated by the onset of absorption is 2.67 eV.



Scheme 5. Reactivity of 7 under Mori's homocoupling conditions.

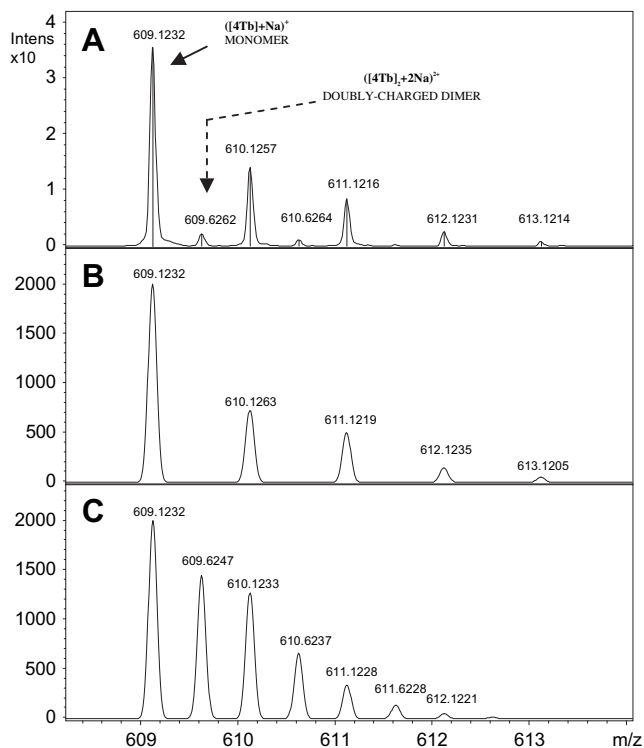


Figure 1. A: experimental HRMS (ESI) of **4Tb**. The arrows point to the signals attributable to the monomeric $[(4Tb)+Na]^+$ ion (all ^{12}C , all ^{32}S -isotopomer) and to the dimeric $[(4Tb)_2+2Na]^{2+}$ ion (one ^{13}C -isotopomer or one ^{33}S -isotopomer); B: calculated isotope pattern of the monomer $[(4Tb)+Na]^+$; C: calculated isotope pattern of the dimer $[(4Tb)_2+2Na]^{2+}$.

In the solid state, the absorption band of **4Ta** is strongly blue-shifted and shows a maximum located at 350 nm with two shoulders at 421 and 458 nm. The blue shift of the absorption maxima in the solid state has already been observed for α -oligothiophenes²⁸ and has been ascribed to the formation of H-aggregates showing the interacting molecules arranged with their long axes parallel to each other.²⁹

Concerning the PL features, the emissions of **4Ta–c** are substantially red shifted and quenched in the solid state further supporting the occurrence of an H-type aggregation.³⁰

Analogous considerations can be drawn for the solution optical properties of **4Td–f** (Fig. 2b) the UV–vis absorption maxima of which fall to 455 nm. The photoluminescence spectra in solution also show a fine structure, although less resolved compared to **4Ta–c**, with the maximum located at 528 nm, followed by a vibronic replica at 561 nm. The Stokes shift of **4Td–f** is slightly lower than

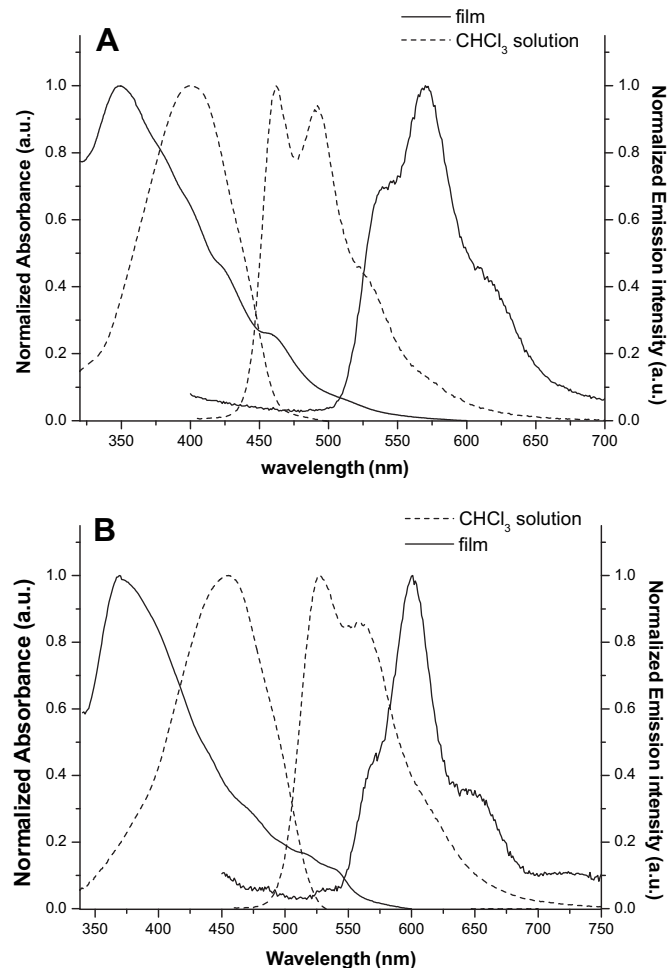


Figure 2. A: Normalized UV–vis absorption and emission spectra of **4Ta** in diluted $CHCl_3$ solution and as film on quartz; B: Normalized UV–vis absorption and emission spectra of **4Td** in diluted $CHCl_3$ solution and as film on quartz.

that of **4Ta–c**. The quantum yields in solution of **4Td–f** are much higher than those obtained for **4Ta–c** and these values are unexpectedly high for thiophene-based materials.

The optical properties of **4Tg** are reported in Figure 3. In diluted $CHCl_3$ solution, the absorption maximum falls to 436 nm, which is slightly blue-shifted with respect to the λ_{max} of the vinylene functionalized **4Td–f** due to the lower degree of conjugation of the

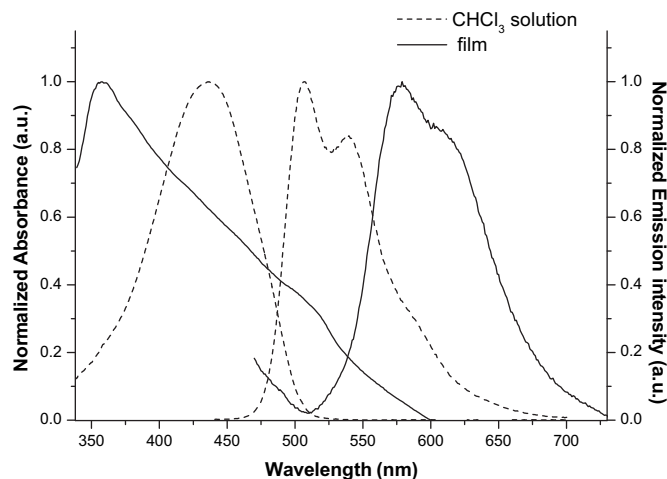


Figure 3. Normalized absorption and emission spectra of **4Tg** in diluted $CHCl_3$ solution and as film on quartz.

Table 1
Optical properties of **4Ta–g**

4T	CHCl ₃ solution					Solid state	
	λ_{abs} (nm)	λ_{em}^a (nm)	Stokes shift ^b (eV)	E_g^{opt} ^c (eV)	Q.Y. (Φ)	λ_{abs}^a (nm)	λ_{em}^a (nm)
4Ta	400	462*, 491, 522	0.42	2.67	0.41	350*, 421, 458	539, 570*, 608
4Tb	400	462*, 491, 522	0.42	2.67	0.42	350*, 421, 458	539, 570*, 608
4Tc	400	462*, 491, 522	0.42	2.67	0.43	350*, 421, 458	539, 570*, 608
4Td	455	528*, 561	0.38	2.37	0.91	369	592, 601*
4Te	455	528*, 561	0.38	2.37	0.88	369	592, 601*
4Tf	455	528*, 561	0.38	2.37	0.89	369	592, 601*
4Tg	436	507*, 539	0.40	2.46	0.70	361	579*, 602

^a The λ_{max} is indicated by an asterisk.

^b Estimated as the difference between λ_{abs} and λ_{em} .

^c Evaluated from the onset of the absorption spectrum in chloroform.

ethynylene with respect to the vinylene groups. The photoluminescence spectrum in solution of **4Tg** also shows a fine structure, with the maximum located to 507 nm, followed by a vibronic replica at 539 nm and its quantum yield in solution falls between those obtained for **4Ta–c** and **4Td–f**.

A good thermal stability (evaluated by the decomposition temperatures at 5% weight loss) for compounds **4Ta–g** was revealed by thermal gravimetric analysis (TGA). Decomposition temperatures range from 310 to 373 °C (Fig. 4), and are significantly higher than those of quaterthiophene³¹ and dialkylquaterthiophene.²⁷ These values rule out the possibility of temperature decarboxylative decompositions^{7f,14b} under the conditions typically employed for the thermal evaporation of semiconductors for the construction of OTFT.

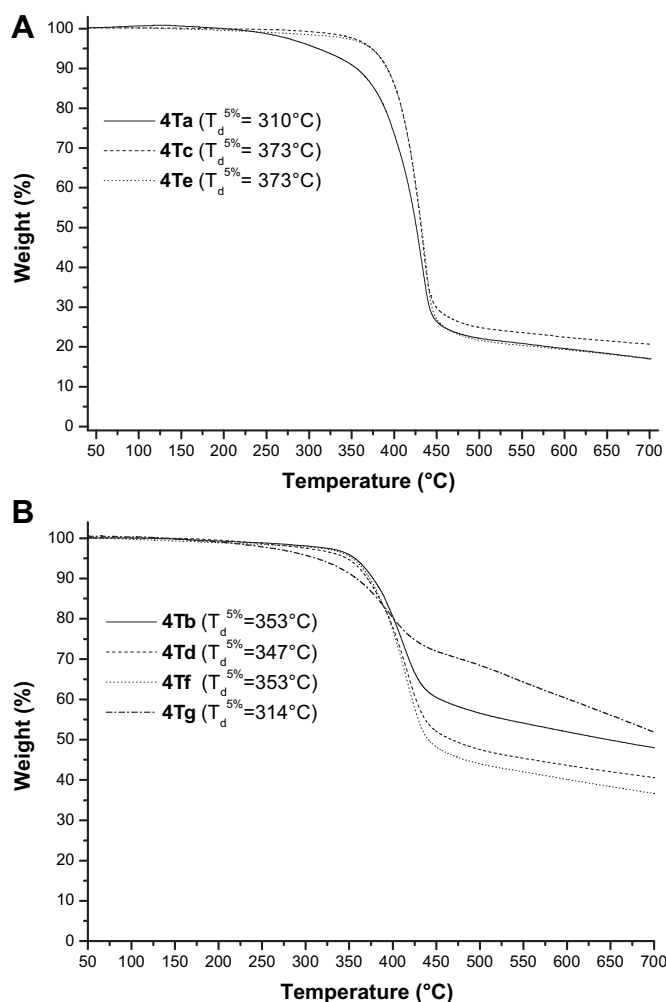


Figure 4. A: TGA traces of **4Ta–c**; B: TGA traces of **4Td–g**.

2.3. Electrochemical properties

The electrochemical properties of **4Ta–g** were investigated by cyclic voltammetry (CV) in order to gain insights into the effects exerted by both the core and the kind of side-chain substituent on the HOMO–LUMO energy levels of quaterthiophenes. The obtained results are summarized in Table 2.

The voltammograms of **4Ta–g** are characterized by the presence, in all cases, of two successive one-electron oxidation waves, the first reversible and the second one quasi-reversible, which can be ascribed to the successive formation of a radical cation and of a dication. Taking -4.8 eV as the HOMO level for the ferrocene redox system³² the HOMO levels of **4Ta–g** could be estimated by

Table 2
Electrochemical properties of **4Ta–g**

4T	$E_{1/2}^{ox}$ (V) ^a	HOMO (eV) ^b	LUMO (eV) ^c
4Ta	0.37	−5.17	−2.50
4Tb	0.44	−5.24	−2.60
4Tc	0.44	−5.24	−2.60
4Td	0.55	−5.35	−2.98
4Te	0.55	−5.35	−2.98
4Tf	0.57	−5.37	−3.00
4Tg	0.67	−5.47	−3.01

^a Half-wave oxidation potential vs Fc/Fc⁺.

^b HOMO = $-(4.8 + E_{1/2}^{ox})$ [eV].

^c LUMO = HOMO + (E_g^{opt}).

the half-wave oxidation potential.³³ The LUMO levels for **4Ta–g** were obtained from the optical energy gaps reported in Table 1 as HOMO + (E_g^{opt}).

The HOMO levels of **4Ta–c** match well with the work function of gold (-5.1 eV) and this could be a favourable prerequisite for facilitating the hole charge injection from the electrode to the organic layer in the OTFT devices. For **4Td–f** and for **4Tg** it is worth noting that both their HOMO and LUMO energy levels are stabilized with respect to those of **4Ta–c**. This stabilization is stronger for the LUMO due to the effect of conjugation between the quaterthiophene core and the carbonyl group.³⁴

2.4. OTFT characterization

The semiconducting properties of the quaterthiophenes **4Ta–g** were investigated by fabricating OTFT devices in top contact configuration. The transistor characteristics were measured by polarizing the devices up to -100 V and, since *p*-type behavior was expected, negative source-drain and gate voltage biases were applied. For preliminary transistor measurement, the active layers of **4Ta–g** were spin coated from 2 mg mL^{-1} chloroform solutions without further thermal treatment. The field-effect mobility (μ), the on/off ratio (I_{on}/I_{off}) and the threshold voltage (V_{th}) extracted for these devices are reported in Table 3. While no appreciable modulation was recorded for **4Td–g**, all devices based on the oligomers **4Ta–c** showed an average μ in the range between 8×10^{-4} and $1.6 \times 10^{-3} \text{ cm}^2 \text{ V}^{-1} \text{ s}^{-1}$ with on/off ratios higher than 10^3 in all cases.

Table 3
OTFT figures of merit obtained for **4Ta–c**

4T	Deposition method ^a	Best μ ($\text{cm}^2 \text{ V}^{-1} \text{ s}^{-1}$)	Average μ^b ($\text{cm}^2 \text{ V}^{-1} \text{ s}^{-1}$)	V_{th}^b (V)	I_{on}/I_{off}
4Ta	I	1.1×10^{-3}	$(8.0 \pm 3.0) \times 10^{-4}$	-15 ± 9	3.8×10^3
4Ta	II	1.5×10^{-3}	$(1.3 \pm 0.1) \times 10^{-3}$	-6.8 ± 1.8	1.1×10^4
4Ta	III	1.5×10^{-3}	$(1.4 \pm 0.1) \times 10^{-3}$	-22 ± 6	4.6×10^3
4Tb	I	1.3×10^{-3}	$(1.1 \pm 0.1) \times 10^{-3}$	-11 ± 3	3.8×10^3
4Tb	II	2.5×10^{-3}	$(2.3 \pm 0.1) \times 10^{-3}$	-17 ± 10	5.9×10^3
4Tb	III	7.0×10^{-3}	$(6.0 \pm 1.0) \times 10^{-3}$	-10 ± 4	6.0×10^3
4Tc	I	1.8×10^{-3}	$(1.6 \pm 0.5) \times 10^{-3}$	-11 ± 6	5.7×10^3
4Tc	II	3.6×10^{-3}	$(2.7 \pm 0.5) \times 10^{-3}$	-13 ± 5	1.7×10^4
4Tc	III	5.5×10^{-3}	$(4.9 \pm 0.6) \times 10^{-3}$	-13 ± 5	1.2×10^4

^a I: spin-coating; II: spin-coating and annealing at 100 °C; III: thermal evaporation.

^b The statistics was carried out on 10 devices.

In order to remove solvent traces from the active layer, another series of devices was constructed where the active layer was subjected to a vacuum annealing of the film at 100 °C for 30 min. As a result, the field effect mobility was increased by a factor of ~ 2 while the on/off ratio was only slightly raised. Figure 5 reports the best $I_{ds}-V_{ds}$ output characteristics along with the I_{ds} and $I_{ds}^{1/2}$ versus V_g plots of a **4Tc**-based OTFT showing the highest performance in terms of both mobility ($3.6 \times 10^{-3} \text{ cm}^2 \text{ V}^{-1} \text{ s}^{-1}$) and on/off ratios (1.7×10^4).

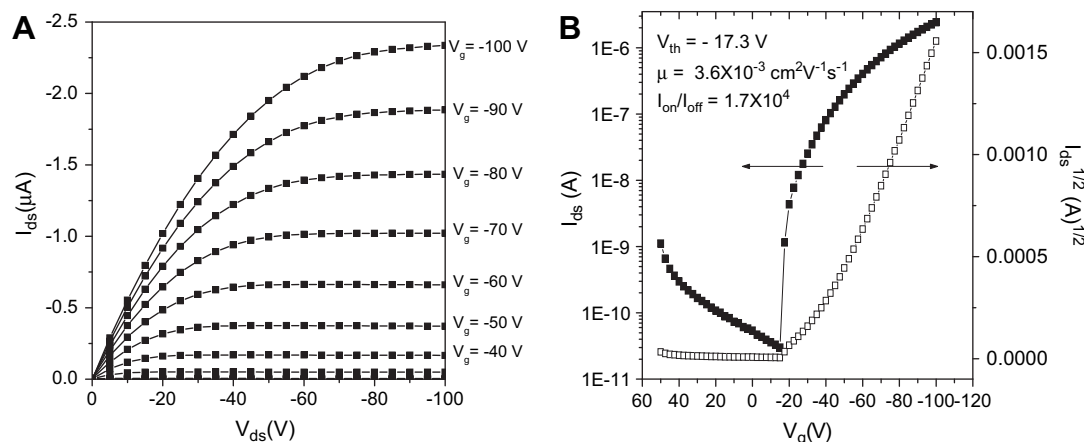


Figure 5. A: I_{ds} – V_{ds} current–voltage characteristics; B: plots of I_{ds} and $I_{ds}^{1/2}$ versus V_g of a solution processed 4Tc-based OTFT.

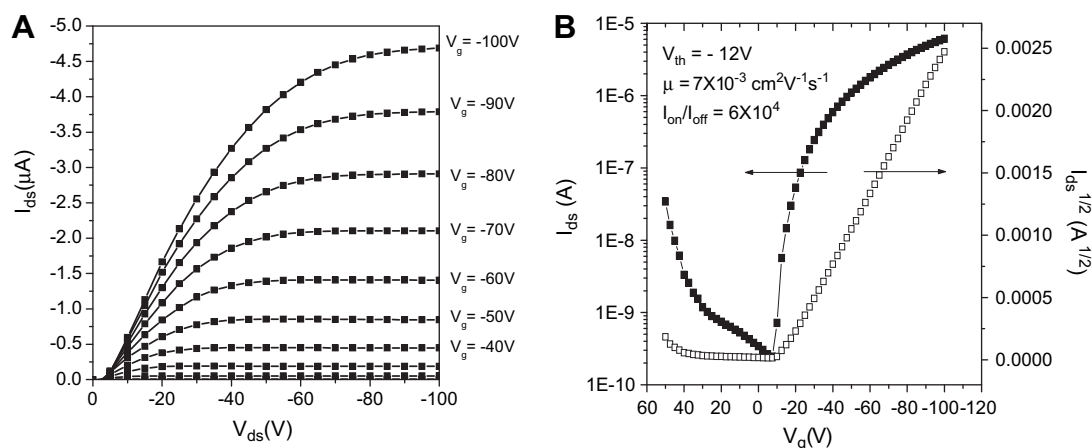


Figure 6. A: I_{ds} – V_{ds} current–voltage characteristics; B: plots of I_{ds} and $I_{ds}^{1/2}$ versus V_g of a thermally evaporated 4Tb-based OTFT.

The good thermal stability of all quaterthiophenes described here, allowed us to deposit 4Ta–c also by thermal evaporation on a Si/SiO₂ substrate.³⁵ All devices showed μ higher than $2 \times 10^{-3} \text{ cm}^2 \text{ V}^{-1} \text{ s}^{-1}$ and on/off ratios higher than 10^3 . The oligomer 4Tb reaches the highest mobility of $7 \times 10^{-3} \text{ cm}^2 \text{ V}^{-1} \text{ s}^{-1}$. The output characteristics, along with the plots of I_{ds} and $I_{ds}^{1/2}$ versus V_g of the relevant device are reported in Figure 6.

3. Conclusions

New soluble quaterthiophenes 4Ta–g in which a quaterthiophene core is bonded to ester groups in the α,ω -terminal positions by means of ethylene (4Ta–c), vinylene (4Td–f) or ethynylene (4Tg) spacers were prepared. The key synthetic step consisted of a Pd-catalyzed homocoupling of suitable bithiophene precursors via a AgF-promoted C–H bond activation which was fully successful for the preparation of 4Ta–f but that suffered from competitive hydrofluorination of the activated C≡C triple bond. Since β -fluoroalkenes are interesting compounds for their potential applications in medicinal chemistry,³⁶ their generation by a stereoselective addition of HF to activated alkynes might be synthetically exploitable.

Thin-films of compound 4Ta–c deposited by spin-coating resulted in OTFTs, which showed hole field-effect mobilities up to $3.6 \times 10^{-3} \text{ cm}^2 \text{ V}^{-1} \text{ s}^{-1}$. Only slightly better mobilities (up to $7 \times 10^{-3} \text{ cm}^2 \text{ V}^{-1} \text{ s}^{-1}$) were obtained by thermal evaporation of the active layer onto Si/SiO₂ substrates. The obtained OTFT figures of merit are remarkable, considering that no device optimization was

performed.³⁷ Further optimization of the devices based on 4Ta–c and their use as chemically selective OTFT sensors are underway.

4. Experimental section

4.1. General remarks, materials and methods

All syntheses were carried out under dry inert nitrogen atmosphere using Schlenk techniques unless otherwise specified. The solvents were carefully dried and freshly distilled prior to use according to common laboratory practice.³⁸ The preparation of 5-bromo-2,2'-bithiophene,³⁹ 5-iodo-2,2'-bithiophene,⁴⁰ bithiophene derivatives 1 and 2,^{7h} PdCl₂(PhCN)₂,⁴¹ PdCl₂(PPh₃)₂,⁴² and Pd(PPh₃)₄⁴³ was carried out according to literature procedures. All other chemicals were purchased from commercially available sources and used without further purifications. Flash column chromatography was performed using Merck Kieselgel 60 (230–400 mesh) silica gel. ¹H NMR, ¹³C{¹H} NMR and ¹⁹F NMR spectra were recorded on a Bruker Avance 400 spectrometer and are reported in ppm which are referenced to Me₄Si (¹H and ¹³C), and CFCl₃ (¹⁹F). FTIR spectra were recorded on a Bruker Vector 22 spectrophotometer. UV–vis spectra were measured with a Shimadzu UV-1601 spectrophotometer and fluorescence spectra were obtained on a Varian Cary Eclipse spectrofluorimeter. Quantum yields were measured by the optically dilute method⁴⁴ using 9,10-diphenylanthracene as standard ($\Phi=0.90$ in cyclohexane).⁴⁵ Cyclic voltammetry measurements were carried out at 25 °C in CHCl₃

solution containing 0.1 M tetrabutylammonium perchlorate (TBAP) as supporting electrolyte with a glassy carbon working electrode on an Autolab potentiostat PGSTAT 10 using a three-electrode cell. The oxidation potentials were measured versus Ag/Ag⁺ as the pseudoreference electrode. The experiments were calibrated with the standard ferrocene/ferrocenium redox couple.⁴⁶ The evaluation of the HOMO level of the polymers was carried out by measuring the half-wave oxidation potential in the anodic scan. GC–MS data (EI, 70 eV) were acquired on a HP 6890 instrument equipped with a HP-5MS capillary column (crosslinked 5% Ph Me siloxane: 30.0 m × 250 μm × 0.25 mm) coupled with a HP 5973 mass spectrometer operating at 70 eV (electron impact). The high resolution mass spectrometry (HRMS) analysis of oligothiophenes was performed using a time-of-flight mass spectrometer equipped with an electrospray ion source (Bruker microTOF) in positive ion mode. The sample solutions (CHCl₃/CH₃OH) were introduced by continuous infusion at a flow rate of 180 μL min⁻¹ with the aid of a syringe pump. The instrument was operated with end-plate offset and capillary voltages set to -500 and -4500 V, respectively. The nebulizer pressure was 0.8 bar (N₂), and the drying gas (N₂) flow rate was 7.0 L min⁻¹. The capillary exit and skimmer 1 voltages were 90 and 30 V, respectively. The drying gas temperature was set at 220 °C. The software used for the simulations was Bruker Daltonics DataAnalysis (version 3.3). The calibration was carried out with sodium formate. Thermogravimetric analyses (TGA) were performed under a nitrogen atmosphere (flow of 40 mL min⁻¹) with a Perkin–Elmer Pyris 6 TGA in the range from 30 to 700 °C with a heating rate of 10 °C min⁻¹. Elemental analyses were performed using a VARIO MICRO-CHNSO Elemental Analyzer.

4.2. Synthetic procedures

4.2.1. Butyl (2E)-3-(2,2'-bithien-5-yl)-propenoate (3). Butyl acrylate (1.332 g, 10.394 mmol), triethylamine (2.10 g, 22.79 mmol), Pd(AcO)₂ (16.8 mg, 0.074 mmol) and P(o-Tol)₃ (91.3 mg, 0.30 mmol) were added to a solution of 5-bromo-2,2'-bithiophene (1.820 g, 7.424 mmol) in anhydrous DMF (12 mL). The reaction mixture was heated at 120 °C and kept under stirring overnight. After cooling to room temperature, the mixture was poured into water (50 mL) and extracted with diethyl ether (3 × 100 mL). The organic layers were collected, washed with water (150 mL), dried over anhydrous Na₂SO₄, filtered, and concentrated under reduced pressure. The residue was purified by flash column chromatography (silica gel, petroleum ether bp 40–60 °C/CH₂Cl₂=3/2) to afford **3** (1.14 g, 65%) as yellow oil. ¹H NMR (400 MHz, CDCl₃): δ 7.73 (d, J=15.6 Hz, 1H), 7.29 (dd, J₁=5.1 Hz, J₂=1.2 Hz, 1H), 7.25 (dd, J₁=3.6 Hz, J₂=1.2 Hz, 1H), 7.16 (d, J=3.8 Hz, 1H), 7.12 (d, J=3.8 Hz, 1H), 7.06 (dd, J₁=5.1 Hz, J₂=3.6 Hz, 1H), 6.20 (d, J=15.6 Hz, 1H), 4.21 (t, J=6.7 Hz, 2H), 1.70 (m, 2H), 1.45 (m, 2H), 0.98 (t, J=7.3 Hz, 3H); ¹³C{¹H} NMR (100.6 MHz, CDCl₃): δ 167.1, 140.3, 138.2, 136.9, 136.8, 132.2, 128.2, 125.7, 124.8, 124.4, 116.7, 64.5, 30.9, 19.3, 13.9. FTIR (neat) ν [cm⁻¹]: 3110, 3074, 3029, 2958, 2928, 2895, 2873, 2867, 1713, 1700, 1624, 1618, 1545, 1505, 1475, 1454, 1425, 1388, 1367, 1354, 1329, 1302, 1274, 1228, 1202, 1169–1160, 1127, 1057, 1047, 1033, 998–988, 960, 898, 890, 857, 842, 809, 702, 693. MS (EI, 70 eV): m/z 292 (M⁺, 100), 236 (58), 219 (64), 192 (78). Anal. Calcd for C₁₅H₁₆O₂S₂: C, 61.61; H, 5.52; S, 21.93. Found: C, 61.37; H, 5.55; S, 21.84.

4.2.2. Butyl 3-(2,2'-bithien-5-yl)-propanoate (4). A solution of **3** (725 mg, 2.48 mmol) in MeOH (50 mL) was slowly added to 264 mg (0.248 mmol) of supported Pd (10%_w on activated charcoal), in a stainless-steel autoclave equipped with a transducer for online pressure monitoring. The autoclave was purged three times with hydrogen, pressurized at constant pressure of 30 atm, and set on a magnetic stirrer. The substrate conversion was monitored by GC–MS. After reaction completion, the mixture was filtered through

a short plug of Celite® and the filtrate was evaporated under reduced pressure. The residue was purified by flash column chromatography (silica gel, petroleum ether bp 40–60 °C/CH₂Cl₂=3/2) to afford **4** (716 mg, 98%) as pale yellow oil. ¹H NMR (400 MHz, CDCl₃): δ 7.19 (dd, J₁=5.1 Hz, J₂=0.9 Hz, 1H), 7.11 (dd, J₁=3.5 Hz, J₂=0.9 Hz, 1H), 7.02–6.98 (m, 2H), 6.74 (br d, J=3.6 Hz, 1H), 4.12 (t, J=6.7 Hz, 2H), 3.15 (t, J=7.5 Hz, 2H), 2.70 (t, J=7.5 Hz, 2H), 1.63 (m, 2H), 1.38 (m, 2H), 0.94 (t, J=7.3 Hz, 3H); ¹³C{¹H} NMR (100.6 MHz, CDCl₃): δ 172.5, 142.5, 137.7, 135.6, 127.8, 125.5, 124.0, 123.5, 123.3, 64.7, 36.0, 30.7, 25.5, 19.2, 13.8. FTIR (neat) ν [cm⁻¹]: 3112, 3074, 2961, 2927, 2869, 1733, 1520, 1469–1427, 1385, 1352, 1257, 1173, 1124, 1084, 1064, 840, 799, 693. MS (EI, 70 eV): m/z 294 (M⁺, 49), 237 (22), 192 (39), 179 (100). Anal. Calcd for C₁₅H₁₈O₂S₂: C, 61.19; H, 6.16; S, 21.78. Found: C, 61.01; H, 6.19; S, 21.71.

4.2.3. Hexyl (2E)-3-(2,2'-bithien-5-yl)-propenoate (5). Following the procedure reported for compound **3**, compound **5** was prepared using 1.998 g (8.150 mmol) of 5-bromo-2,2'-bithiophene, 1.782 g (11.410 mmol) of hexyl acrylate, 2.310 g (22.828 mmol) of triethylamine, 18.3 mg (0.0815 mmol) of Pd(AcO)₂, 99.2 mg (0.326 mmol) of P(o-Tol)₃, and 14 mL of anhydrous DMF, respectively. The crude product was purified by flash column chromatography (silica gel, petroleum ether bp 40–60 °C/CH₂Cl₂=4/1) to afford **5** (1.83 g, 70%) as yellow oil. ¹H NMR (400 MHz, CDCl₃): δ 7.73 (d, J=15.6 Hz, 1H), 7.29 (dd, J₁=5.1 Hz, J₂=0.9 Hz, 1H), 7.24 (dd, J₁=3.6 Hz, J₂=0.9 Hz, 1H), 7.16 (d, J=3.8 Hz, 1H), 7.12 (d, J=3.8 Hz, 1H), 7.05 (dd, J₁=5.1 Hz, J₂=3.6 Hz, 1H), 6.20 (d, J=15.6 Hz, 1H), 4.20 (t, J=6.7 Hz, 2H), 1.70 (m, 2H), 1.46–1.30 (br m, 6H), 0.98 (t, J=6.8 Hz, 3H). ¹³C{¹H} NMR (100.6 MHz, CDCl₃): δ 167.1, 140.3, 138.2, 136.9, 136.8, 132.2, 128.2, 125.7, 124.8, 124.4, 116.7, 64.8, 31.6, 28.8, 25.7, 22.7, 14.2. FTIR (neat) ν [cm⁻¹]: 3110, 3073, 2960, 2929, 2870, 2858, 1713, 1622, 1548, 1506, 1454, 1425, 1386, 1369, 1353, 1303, 1269, 1223, 1201, 1167, 1080, 1050, 1020, 970, 890, 842, 795, 695. MS (EI, 70 eV): m/z 320 (M⁺, 100), 236 (81), 219 (67), 192 (83). Anal. Calcd for C₁₇H₂₀O₂S₂: C, 63.71; H, 6.29; S, 20.01. Found: C, 63.52; H, 6.31; S, 19.93.

4.2.4. Hexyl 3-(2,2'-bithien-5-yl)-propanoate (6). Compound **6** was prepared as pale yellow oil following the procedure reported for **4** using 770 mg (2.40 mmol) of **5**, 256 mg (0.24 mmol) of supported Pd (10%_w on activated charcoal), and 48 mL of MeOH, respectively. Yield: 736 mg (95%). ¹H NMR (400 MHz, CDCl₃): δ 7.19 (dd, J₁=5.2 Hz, J₂=0.9 Hz, 1H), 7.11 (dd, J₁=3.5 Hz, J₂=0.9 Hz, 1H), 7.02–6.98 (m, 2H), 6.74 (br d, J=3.6 Hz, 1H), 4.11 (t, J=6.7 Hz, 2H), 3.15 (t, J=7.5 Hz, 2H), 2.71 (t, J=7.5 Hz, 2H), 1.63 (m, 2H), 1.29–1.25 (br m, 6H), 0.90 (t, J=7.0 Hz, 3H); ¹³C{¹H} NMR (100.6 MHz, CDCl₃): δ 172.5, 142.5, 137.7, 135.6, 127.8, 125.5, 124.1, 123.5, 123.3, 64.7, 36.0, 31.5, 28.6, 25.7, 25.5, 22.6, 14.1. FTIR (neat) ν [cm⁻¹]: 3109, 3071, 2958, 2933, 2872, 2858, 1737, 1519, 1468, 1457, 1428, 1392, 1357, 1297, 1255, 1208, 1174, 1125, 1080, 1051, 910, 887, 840, 799, 694. MS (EI, 70 eV): m/z 322 (M⁺, 68), 237 (40), 192 (48), 179 (100). Anal. Calcd for C₁₇H₂₂O₂S₂: C, 63.61; H, 6.91; S, 19.89. Found: C, 63.36; H, 6.95; S, 19.81.

4.2.5. Ethyl (2,2'-bithien-5-yl)-propynoate (7). 5.7 mL (11.40 mmol) of a 2.0 M THF/hexane solution of LDA was added to a solution of ethyl propynoate (1.120 g, 11.417 mmol) in THF (9 mL) kept at -78 °C and under stirring. After 15 min, 22.8 mL (11.40 mmol) of a 0.5 M THF solution of anhydrous ZnCl₂ was added by a syringe. The solution was gradually warmed to room temperature within 30 min and subsequently transferred via a cannula to a flask containing a mixture of 5-iodo-2,2'-bithiophene (2.404 g, 8.228 mmol), Pd(PPh₃)₄ (0.475 g, 0.411 mmol), and toluene (60 mL). The reaction mixture was subsequently heated at 80 °C and kept under stirring for 4 h. After cooling down to room temperature, diethyl ether (70 mL) and a saturated NH₄Cl solution (100 mL) were added to the reaction mixture. The organic layer was separated, washed with

water, dried over anhydrous Na_2SO_4 , filtered, and concentrated under reduced pressure. The residue was purified by flash column chromatography (silica gel, petroleum ether bp 40–60 °C/ $\text{CH}_2\text{Cl}_2=7/3$) to afford **7** (1693 g, 78%) as yellow solid. Mp=57–58 °C. ^1H NMR (400 MHz, CDCl_3): δ 7.41 (d, $J=4.0$ Hz, 1H), 7.31 (dd, $J_1=5.1$ Hz, $J_2=1.0$ Hz, 1H), 7.26 (dd, $J_1=3.6$ Hz, $J_2=1.0$ Hz, 1H), 7.10 (d, $J=4.0$ Hz, 1H), 7.06 (dd, $J_1=5.1$ Hz, $J_2=3.6$ Hz, 1H), 4.32 (q, $J=7.2$ Hz, 2H), 1.38 (t, $J=7.2$ Hz, 3H). $^{13}\text{C}\{^1\text{H}\}$ NMR (100.6 MHz, CDCl_3): δ 154.0, 143.0, 137.7, 136.0, 128.2, 126.2, 125.3, 123.8, 117.6, 85.9, 80.3, 62.2, 14.2. FTIR (neat) ν [cm^{-1}]: 3118, 3058, 2988, 2943, 2943, 2911, 2853, 2207, 2165, 1707, 1689, 1546, 1535, 1505, 1479, 1455, 1445, 1422, 1391, 1369, 1354, 1322, 1270, 1242, 1224, 1212, 1198, 1169, 1080, 1059, 1047, 1016, 860, 843, 826, 794, 740, 709, 698. MS (EI, 70 eV): m/z 262 (M^+ , 37), 217 (22), 190 (100), 145 (16). Anal. Calcd for $\text{C}_{13}\text{H}_{10}\text{O}_2\text{S}_2$: C, 59.92; H, 3.84; S, 24.45. Found: C, 59.77; H, 3.86; S, 24.35.

4.2.6. Bis-ethyl 3-(2,2':5',2'':5'',2'''-quaterthiophen-5,5'''-diyl)-dipropenoate (4Ta). AgF (589 mg, 4.64 mmol) was added in one portion to a mixture of $\text{PdCl}_2(\text{PhCN})_2$ (27 mg, 0.07 mmol), **2** (618 mg, 2.32 mmol), and DMSO (23 mL). The reaction mixture was allowed to reach 70 °C and kept under stirring for 24 h. It was then cooled to room temperature, diluted with CHCl_3 (100 mL), and filtered through a short plug of Celite® on a sintered glass filter (G3), which was successively washed with other CHCl_3 (200 mL). The filtrate was washed with water (2×100 mL) and brine (100 mL). The organic layer was dried over anhydrous Na_2SO_4 , filtered, and concentrated under reduced pressure. The residue was purified by flash column chromatography (silica gel, $\text{CHCl}_3/\text{hexane}=3/2$) to afford **4Ta** (370 mg, 60%) as yellow solid. ^1H NMR (400 MHz, CDCl_3): δ 7.05 (d, $J=3.8$ Hz, 2H), 7.01 (d, $J=3.8$ Hz, 2H), 6.99 (d, $J=3.6$ Hz, 2H), 6.75 (d, $J=3.6$ Hz, 2H), 4.18 (q, $J=7.2$ Hz, 4H), 3.15 (t, $J=7.5$ Hz, 4H), 2.70 (t, $J=7.5$ Hz, 4H), 1.28 (t, $J=7.2$ Hz, 6H). $^{13}\text{C}\{^1\text{H}\}$ NMR (100.6 MHz, CDCl_3): δ 172.4, 142.8, 136.5, 135.6, 135.3, 125.7, 124.3, 123.9, 123.5, 60.8, 36.0, 25.5, 14.3. FTIR (KBr pellet) ν [cm^{-1}]: 3095, 3075, 3059, 2978, 2917, 2872, 2847, 1729, 1515, 1467, 1442, 1436, 1419, 1395, 1380, 1339, 1303, 1180, 1163, 1098, 1066, 1032, 1019, 1005, 898, 864, 845, 806, 792. HRMS (ESI): m/z calculated for $[\text{C}_{26}\text{H}_{26}\text{O}_4\text{S}_4+\text{Na}]^+$: 553.0606 found: 553.0599. Anal. Calcd for $\text{C}_{26}\text{H}_{26}\text{O}_4\text{S}_4$: C, 58.84; H, 4.94; S, 24.17. Found: C, 58.61; H, 4.96; S, 24.07.

4.2.7. Bis-butyl 3-(2,2':5',2'':5'',2'''-quaterthiophen-5,5'''-diyl)-dipropenoate (4Tb). Compound **4Tb** was synthesized following the procedure reported for **4Ta** using 518 mg (1.76 mmol) of **4**, 20.2 mg (0.052 mmol) of $\text{PdCl}_2(\text{PhCN})_2$, 447 mg (3.52 mmol) of AgF, and 18 mL of DMSO, respectively. The crude product was purified by flash column chromatography (silica gel, petroleum ether bp 40–60 °C/ $\text{CH}_2\text{Cl}_2=1/4$) to afford **4Tb** (264 mg, 51%) as yellow solid. ^1H NMR (400 MHz, CDCl_3): δ 7.05 (d, $J=3.8$ Hz, 2H), 7.01 (d, $J=3.8$ Hz, 2H), 6.99 (d, $J=3.6$ Hz, 2H), 6.75 (d, $J=3.6$ Hz, 2H), 4.12 (t, $J=6.7$ Hz, 4H), 3.15 (t, $J=7.5$ Hz, 4H), 2.71 (t, $J=7.5$ Hz, 4H), 1.63 (m, 4H), 1.38 (m, 4H), 0.94 (t, $J=7.3$ Hz, 6H). $^{13}\text{C}\{^1\text{H}\}$ NMR (100.6 MHz, CDCl_3): δ 172.5, 142.8, 136.5, 135.6, 135.3, 125.7, 124.2, 123.9, 123.5, 64.7, 36.0, 30.7, 25.5, 19.2; 13.8. FTIR (KBr pellet) ν [cm^{-1}]: 3058, 2959, 2934, 2913, 2874, 2847, 1725, 1515, 1468, 1440, 1421, 1396, 1378, 1339, 1305, 1275, 1188, 1170, 1121, 1067, 1018, 1049, 846, 807, 792. HRMS (ESI): m/z calculated for $[\text{C}_{30}\text{H}_{34}\text{O}_4\text{S}_4+\text{Na}]^+$: 609.1232 found: 609.1232. Anal. Calcd for $\text{C}_{30}\text{H}_{34}\text{O}_4\text{S}_4$: C, 61.40; H, 5.84; S, 21.85. Found: C, 61.15; H, 5.69; S, 21.98.

4.2.8. Bis-hexyl 3-(2,2':5',2'':5'',2'''-quaterthiophen-5,5'''-diyl) dipropenoate (4Tc). Compound **4Tc** was synthesized following the procedure described for **4Ta** using 420 mg (1.30 mmol) of **6**, 15 mg (0.039 mmol) of $\text{PdCl}_2(\text{PhCN})_2$, 330 mg (2.60 mmol) of AgF, and 13 mL of DMSO, respectively. The crude product was purified by flash column chromatography (silica gel, petroleum ether bp 40–60 °C/

$\text{CH}_2\text{Cl}_2=1/1$) to afford **4Tc** (247 mg, 59%) as yellow solid. ^1H NMR (400 MHz, CDCl_3): δ 7.05 (d, $J=3.8$ Hz, 2H), 7.01 (d, $J=3.8$ Hz, 2H), 6.99 (d, $J=3.6$ Hz, 2H), 6.75 (d, $J=3.6$ Hz, 2H), 4.11 (t, $J=6.7$ Hz, 4H), 3.15 (t, $J=7.5$ Hz, 4H), 2.71 (t, $J=7.5$ Hz, 4H), 1.63 (m, 4H), 1.39–1.25 (m, 12H), 0.90 (t, $J=7.0$ Hz, 6H). $^{13}\text{C}\{^1\text{H}\}$ NMR (100.6 MHz, CDCl_3): δ 172.5, 142.8, 136.5, 135.6, 135.3, 125.7, 124.2, 123.9, 123.5, 65.0, 36.0, 31.5, 28.6, 25.7, 25.5, 22.6, 14.1. FTIR (KBr pellet) ν [cm^{-1}]: 3095, 3074, 3059, 2955, 2918, 2871, 2857, 1726, 1515, 1505, 1468, 1442, 1437, 1420, 1397, 1378, 1338, 1306, 1275, 1237, 1186, 1172, 1120, 1017, 898, 890, 846, 805, 791. HRMS (ESI): m/z calculated for $[\text{C}_{34}\text{H}_{42}\text{O}_4\text{S}_4+\text{Na}]^+$: 665.1858 found: 665.1857. Anal. Calcd for $\text{C}_{34}\text{H}_{42}\text{O}_4\text{S}_4$: C, 63.51; H, 6.58; S, 19.95. Found: C, 63.48; H, 6.62; S, 19.42.

4.2.9. Bis-ethyl (2E) 3-(2,2':5',2'':5'',2'''-quaterthiophen-5,5'''-diyl)-dipropenoate (4Td). Compound **4Td** was synthesized following the procedure reported for **4Ta** using 561 mg (2.12 mmol) of **1**, 24.5 mg (0.064 mmol) of $\text{PdCl}_2(\text{PhCN})_2$, 538 mg (4.24 mmol) of AgF, and 21 mL of DMSO, respectively. The crude product was purified by flash column chromatography (silica gel, $\text{CHCl}_3/\text{hexane}=3/2$ followed by elution with CHCl_3) to afford **4Td** (363 mg, 65%) as red-orange solid. ^1H NMR (400 MHz, CDCl_3): δ 7.74 (d, $J=15.6$ Hz, 2H), 7.20–7.16 (br m, 4H), 7.15–7.12 (br m, 4H), 6.20 (d, $J=15.6$ Hz, 2H), 4.27 (q, $J=7.1$ Hz, 4H), 1.35 (t, $J=7.1$ Hz, 6H). $^{13}\text{C}\{^1\text{H}\}$ NMR (100.6 MHz, CDCl_3): δ 166.9, 139.7, 138.5, 136.8, 136.8, 135.9, 132.3, 125.6, 124.9, 124.5, 116.9, 60.7, 14.4. FTIR (KBr pellet) ν [cm^{-1}]: 3080, 3072, 3060, 3006, 2983, 2961, 2939, 1711, 1623, 1500, 1452, 1441, 1396, 1367, 1353, 1307, 1253, 1235, 1206, 1192, 1175, 1160, 1097, 1070, 1049, 1027, 974, 869, 849, 804, 791. HRMS (ESI): m/z calculated for $[\text{C}_{26}\text{H}_{22}\text{O}_4\text{S}_4+\text{Na}]^+$: 549.0302 found: 549.0293. Anal. Calcd for $\text{C}_{26}\text{H}_{22}\text{O}_4\text{S}_4$: C, 59.29; H, 4.21; S, 24.35. Found: C 59.11; H 4.23; S 24.25.

4.2.10. Bis-butyl (2E) 3-(2,2':5',2'':5'',2'''-quaterthiophen-5,5'''-diyl)-dipropenoate (4Te). Compound **4Te** was synthesized following the procedure described for **4Ta** using 439 mg (1.50 mmol) of **3**, 17.3 mg (0.045 mmol) of $\text{PdCl}_2(\text{PhCN})_2$, 381 mg (3.00 mmol) of AgF, and 15 mL of DMSO, respectively. The crude product was purified by flash column chromatography (silica gel, petroleum ether bp 40–60 °C/ $\text{CH}_2\text{Cl}_2=1/4$) to afford **4Te** (315 mg, 72%) as red-orange solid. ^1H NMR (400 MHz, CDCl_3): δ 7.73 (d, $J=15.6$ Hz, 2H), 7.20–7.11 (br m, 8H), 6.21 (d, $J=15.6$ Hz, 2H), 4.22 (t, $J=6.7$ Hz, 4H), 1.70 (m, 4H), 1.45 (m, 4H), 0.98 (t, $J=7.3$ Hz, 6H). $^{13}\text{C}\{^1\text{H}\}$ NMR (100.6 MHz, CDCl_3): δ 167.0, 139.7, 138.6, 136.7, 135.9, 132.3, 125.6, 124.9, 124.5, 116.9, 64.6, 30.9, 19.3, 13.9. FTIR (KBr pellet) ν [cm^{-1}]: 3080, 3072, 3061, 2960, 2935, 2874, 1711, 1625, 1541, 1501, 1468, 1441, 1396, 1354, 1306, 1255, 1236, 1207, 1194, 1163, 1118, 1071, 1050, 1010, 972, 918, 900, 875, 849, 806, 792. HRMS (ESI): m/z calculated for $[\text{C}_{30}\text{H}_{30}\text{O}_4\text{S}_4+\text{Na}]^+$: 605.0919 found: 605.0903. Anal. Calcd for $\text{C}_{30}\text{H}_{30}\text{O}_4\text{S}_4$: C, 61.82; H, 5.19; S, 22.01. Found: C 62.01; H 5.23; S 21.89.

4.2.11. Bis-hexyl (2E) 3-(2,2':5',2'':5'',2'''-quaterthiophen-5,5'''-diyl) dipropenoate (4Tf). Compound **4Tf** was synthesized following the procedure described for **4Ta** using 660 mg (2.06 mmol) of **5**, 24 mg (0.062 mmol) of $\text{PdCl}_2(\text{PhCN})_2$, 523 mg (4.12 mmol) of AgF, and 20 mL of DMSO, respectively. The crude product was purified by flash column chromatography (silica gel, petroleum ether bp 40–60 °C/ $\text{CH}_2\text{Cl}_2=1/6$) to afford **4Tf** (415 mg, 63%) as red-orange solid. ^1H NMR (400 MHz, CDCl_3): δ 7.73 (d, $J=15.6$ Hz, 2H), 7.19–7.15 (br m, 4H), 7.14–7.11 (br m, 4H), 6.20 (d, $J=15.6$ Hz, 2H), 4.20 (q, $J=6.7$ Hz, 4H), 1.71 (m, 4H), 1.46–1.30 (br m, 12H), 0.92 (t, $J=6.7$ Hz, 6H). $^{13}\text{C}\{^1\text{H}\}$ NMR (100.6 MHz, CDCl_3): δ 167.0, 139.7, 138.5, 136.8, 136.7, 135.9, 132.3, 125.6, 124.9, 124.5, 116.9, 64.9, 31.6, 28.8, 25.7, 22.7, 14.1. FTIR (KBr pellet) ν [cm^{-1}]: 3074, 3062, 3030, 2955, 2927, 2872, 2858, 1717, 1697, 1622, 1541, 1500, 1468, 1441, 1395, 1353, 1329, 1310, 1276, 1252, 1235, 1204, 1191, 1161, 1124, 1070, 1047, 1028, 980, 970, 853, 846, 804, 790. HRMS (ESI): m/z calculated for

[C₃₄H₃₈O₄S₄+Na]⁺: 661.1545 found: 661.1542. Anal. Calcd for: C, 63.82; H, 5.99; S, 20.07. Found: C, 63.63; H, 5.91; S, 19.92.

4.2.12. Ethyl 3-(2,2'-bithien-5-yl)-3-fluoro propenoate (8), Bis-ethyl 3-(2,2':5',2'':5'',2''':5''':5''''-quaterthiophen-5,5''''-diyl) dipropynoate (4Tg), and ethyl (Z) 3-(5''-ethoxycarbonyl ethynyl-[2,2':5',2'':5'',2''':5''':5''''-quaterthiophen-5-yl)-3-fluoro-propenoate (4TgHF) and Bis-ethyl (Z) 3-(2,2':5',2'':5'',2''':5''':5''''-quaterthiophen-5,5''''-diyl)-3-fluoro dipropenoate (4TgH₂F₂). To a mixture of PdCl₂(PhCN)₂ (17.7 mg, 0.0462 mmol), **7** (404 mg, 1.54 mmol), and DMSO (16 mL), was added AgF (391 mg, 3.08 mmol) in one portion. After the addition, the reaction was heated to 70 °C and kept under stirring for 24 h. The mixture was then cooled to room temperature, diluted with CHCl₃ (80 mL), and filtered through a short plug of Celite® on a sintered glass filter (G3), which was successively washed with other CHCl₃ (150 mL). The filtrate was washed with water (2 × 100 mL) and brine (100 mL). The organic layer was dried over anhydrous Na₂SO₄, filtered, and concentrated under reduced pressure. The purification of the residue by flash column chromatography (silica gel, petroleum ether bp 40–60 °C/CH₂Cl₂=7/3, followed by petroleum ether bp 40–60 °C/CH₂Cl₂=1/1, petroleum ether bp 40–60 °C/CH₂Cl₂=3/7 and CH₂Cl₂) afforded 22 mg of **8** (5%; Z/E=96/4) as yellow oil, 12 mg of **4Tg** (3%) as yellow solid, 50 mg of **4TgHF** (12%) as orange solid, and 113 mg of **4TgH₂F₂** (26%) as red solid, respectively. **8**: ¹H NMR (400 MHz, CDCl₃): δ 7.40 (d, J=4.0 Hz, 1H), 7.32 (dd, J₁=5.1 Hz, J₂=1.0 Hz, 1H), 7.26 (dd, J₁=3.6 Hz, J₂=1.0 Hz, 1H), 7.15 (dd, J₁=4.0 Hz, J₂=0.8 Hz, 1H), 7.07 (dd, J₁=5.1 Hz, J₂=3.6 Hz, 1H), 5.76 (d, ³J_{H,F}=24.3 Hz, 1H (E)), 5.69 (d, ³J_{H,F}=32.7 Hz, 1H (Z)), 4.26 (q, J=7.2 Hz, 2H), 1.34 (t, J=7.2 Hz, 3H). ¹³C{¹H} NMR (100.6 MHz, CDCl₃): δ 163.9 (d, ³J_{C(O),F}=2.7 Hz), 161.3 (d, ¹J_{C,F}=273.6 Hz), 141.8, 136.0, 131.7 (d, ³J_{C,F}=32.3 Hz), 129.7 (d, ²J_{C,F}=5.2 Hz), 128.3, 126.27, 125.3, 124.4, 95.8 (d, ²J_{C,F}=6.1 Hz), 60.5, 14.4. ¹⁹F NMR (376.6 MHz, CDCl₃): δ -82.93 (d, ³J_{F,H}=24.3 Hz), -93.20 (d, ³J_{F,H}=32.7 Hz). FTIR (neat) ν [cm⁻¹] 3107, 3075, 2978, 2958, 2926, 1718, 1640, 1549, 1510, 1501, 1456, 1425, 1394, 1371, 1335, 1316, 1271, 1223, 1205, 1155, 1097, 1084, 1069, 1040, 1014, 949, 891, 842, 805, 699. MS (EI, 70 eV): m/z 282 (M⁺, 82), 237 (66), 210 (100), 165 (31). Anal. Calcd for C₁₃H₁₁FO₂S₂: C, 55.30; H, 3.93; S, 22.71. Found: C, 55.14; H, 3.95; S, 22.62. **4Tg**: ¹H NMR (400 MHz, CDCl₃): δ 7.43 (d, J=4.0 Hz, 2H), 7.21 (d, J=3.8 Hz, 2H), 7.16 (d, J=3.8 Hz, 2H), 7.14 (d, J=4.0 Hz, 2H), 4.28 (q, J=7.2 Hz, 4H), 1.34 (t, J=7.2 Hz, 6H). ¹³C{¹H} NMR (100.6 MHz, CDCl₃): δ 153.9, 142.2, 137.6, 135.2, 126.0, 125.0, 123.8, 117.9, 86.1, 80.0, 62.2, 14.1. FTIR (KBr pellet) ν [cm⁻¹] 3094, 3065, 2985, 2938, 2200, 1699, 1437, 1365, 1295, 1249, 1227, 1213, 1194, 1154, 1069, 1053, 1016, 847, 794, 740, 742. HRMS (ESI): m/z calculated for [C₂₆H₁₈O₄S₄+Na]⁺: 544.9980 found: 544.9974. Anal. Calcd for C₂₆H₁₈O₄S₄: C, 59.75; H, 3.47; S, 24.54. Found: C, 60.05; H, 3.50; S, 24.28. **4TgHF**: ¹H NMR (400 MHz, CDCl₃): δ 7.41 (m, 2H), 7.18 (d, J=4.0 Hz, 2H), 7.14 (m, 3H), 7.10 (d, J=4.0 Hz, 1H), 5.70 (d, ³J_{H,F}=32.7 Hz, 1H), 4.32 (q, J=7.2 Hz, 2H), 4.26 (q, J=7.2 Hz, 1H), 1.36 (m, 6H). ¹³C{¹H} NMR (100.6 MHz, CDCl₃): δ 163.8 (d, ³J_{C(O),F}=2.5 Hz), 161.1 (d, ¹J_{C,F}=273.2 Hz), 154.0, 142.3, 141.1, 137.7, 137.2, 137.1, 135.3, 132.0 (²J_{C,F}=32.2 Hz), 129.7 (d, ³J_{C,F}=5.2 Hz), 126.1, 125.1, 125.0, 124.5, 123.8, 118.0, 96.1 (d, ²J_{C,F}=6.1 Hz), 86.2, 80.1, 62.3, 60.6, 14.4, 14.2. ¹⁹F NMR (376.6 MHz, CDCl₃): δ -93.20 (d, ³J_{F,H}=32.7 Hz). FTIR (KBr pellet) ν [cm⁻¹] 3095, 3077, 3066, 3051, 2980, 2936, 2905, 2202, 1701, 1638, 1541, 1521, 1501, 1451, 1439, 1391, 1368, 1352, 1331, 1289, 1277, 1252, 1232, 1218, 1204, 1195, 1159, 1097, 1069, 1050, 1019, 940, 848, 795, 745. HRMS (ESI): m/z calculated for [C₂₆H₁₉O₄S₄F+Na]⁺: 565.0042 found: 565.0040. Anal. Calcd for C₂₆H₁₉O₄S₄F: C, 57.54; H, 3.53; S, 23.63. Found: C, 57.89; H, 3.61; S, 23.44. **4TgH₂F₂**: ¹H NMR (400 MHz, CDCl₃): δ 7.40 (d, J=4.0 Hz, 2H), 7.17 (d, J=4.0 Hz, 2H), 7.13 (m, 4H), 5.70 (d, ³J_{H,F}=32.7 Hz, 2H), 4.26 (q, J=7.2 Hz, 4H), 1.34 (t, J=7.2 Hz, 6H). ¹³C{¹H} NMR (100.6 MHz, CDCl₃): δ 163.8 (d, ³J_{C(O),F}=2.5 Hz), 161.0 (d, ¹J_{C,F}=273.3 Hz), 141.1, 137.1, 135.3, 132.0 (²J_{C,F}=32.2 Hz), 129.7 (³J_{C,F}=5.3 Hz), 126.1, 125.1, 124.5, 96.1 (²J_{C,F}=6.1 Hz), 60.6, 14.4. ¹⁹F NMR (376.6 MHz, CDCl₃): δ -93.20 (d, ³J_{F,H}=32.7 Hz). FTIR (KBr pellet) ν [cm⁻¹] 3091, 3077, 3063, 3052, 2980, 2935, 2904, 2871, 1700, 1642, 1542, 1451, 1441, 1394, 1368, 1336, 1320, 1268, 1230, 1195, 1156, 1095, 1075, 1046, 1014, 940, 848, 792,

784. HRMS (ESI): m/z calculated for [C₂₆H₂₀O₄S₄F₂+Na]⁺: 585.0105 found: 585.0101. Anal. Calcd for C₂₆H₂₀O₄S₄F₂: C, 55.50; H, 3.58; S, 22.79. Found: C, 55.85; H, 3.87; S, 22.57.

4.3. Device fabrication

Organic thin film transistors were fabricated in 'top contact' configuration. The devices are constituted by a heavily *n*-doped silicon substrate (resistivity: 0.02–1 Ω cm) coated by a thermally grown 300 nm thick SiO₂ oxide layer (C_i=10 nF cm⁻²). All Si/SiO₂ substrates were cleaned as follows: the substrates were rinsed with deionized water, acetone, deionized water and dried in nitrogen flow. Subsequently they were sonicated in isopropanol for 10 min and then washed again with a further step water/acetone/water and dried again with nitrogen. Finally the substrates were sonicated in methanol for 10 min and rinsed with the last water/acetone/water washing step and dried with nitrogen flow. A gold ohmic contact created directly on the silicon substrate works as the gate contact. Films of **4Ta–g** were deposited on the substrate either by spin-coating from anhydrous CHCl₃ solutions (2 mg mL⁻¹) at 2000 rpm for 30 s or by vacuum sublimation (10⁻⁶ Torr). The spin coated thin films were also annealed at 100 °C for 30 min in high vacuum condition (10⁻⁵ Torr). The film thicknesses were measured by a KLA Tencor T10 profilometer and were found to be 50 nm for vacuum deposited films and 30 nm for spin-coated films. The drain and source electrodes were fabricated on the organic semiconducting layer by gold thermal evaporation through a shadow mask. The resulting channel dimensions were L=200 μm and W=4 mm. The I_{ds}–V_{ds} current–voltage characteristics were evaluated by an Agilent 4155B semiconductor parameter analyzer operating the device in a common source configuration and in the accumulation mode. The V_{ds} and V_g potentials ranged between 0 V and –100 V. The field-effect mobility (μ) and the threshold voltage (V_{th}), in saturation regimes (V_{ds}>V_g), were extracted using the equation:

$$\sqrt{I_{ds}} = \sqrt{\left(C_i \mu \frac{W}{2L}\right)} (V_g - V_{th})$$

where I_{ds} is the drain-source current, C_i is the capacitance per unit area of the gate dielectric layer, V_g is the gate voltage.

Acknowledgements

The assistance of Mr. L. Rutigliano in the preparation of the quaterthiophenes and of Ms M.D. Angione in carrying out OTFT electrical characterization is gratefully acknowledged.

Supplementary data

This section contains copies of NMR spectra for all new compounds described in this paper. Supplementary data associated with this article can be found in online version, at doi:10.1016/j.tet.2009.09.065.

References and notes

- (a) Murphy, A. R.; Fréchet, J. M. J. *Chem. Rev.* **2007**, *107*, 1066–1096; (b) Facchetti, A. *Mater. Today* **2007**, *10*, 28–37; (c) *Organic Electronics: Materials, Manufacturing and Applications*; Klauk, H., Ed.; Wiley-VCH: Weinheim, Germany, 2006; (d) Anthony, J. E. *Chem. Rev.* **2006**, *106*, 5028–5048.
- Horowitz, G.; Fichou, D.; Peng, X.; Xu, Z.; Garnier, F. *Solid State Commun.* **1989**, *72*, 381–384.
- (a) Garnier, F.; Yassar, A.; Hajlaoui, R.; Horowitz, G.; Deloffre, F.; Servet, B.; Ries, S.; Alnot, P. *J. Am. Chem. Soc.* **1993**, *115*, 8716–8721; (b) Bäuerle, P. Sulfur-containing oligomers In *Electronic Materials: The Oligomeric Approach*; Müllen, K., Wegner, G., Eds.; Wiley-VCH: Weinheim, Germany, 1998; pp 105–197; (c) *Handbook of Oligo and Polythiophenes*; Fichou, D., Ed.; Wiley-VCH: Weinheim, Germany, 1999; (d) Katz, H. E.; Bao, Z.; Gilat, S. L. *Acc. Chem. Res.*

- 2001, 34, 359–369; (e) Haliq, M.; Klauk, H.; Zschieschang, U.; Schmid, G.; Ponomarenko, S.; Kirchmeyer, S.; Weber, W. *Adv. Mater.* **2003**, 15, 917–922.
4. Mishra, A.; Ma, C.-Q.; Bäuerle, P. *Chem. Rev.* **2009**, 109, 1141–1276.
5. For reviews see: (a) Roberts, M. E.; Sokolov, A. N.; Bao, Z. *J. Mater. Chem.* **2009**, 19, 3351–3363; (b) Torsi, L.; Tanese, M. C.; Crone, B.; Deepak, S.; Dodabalapur, A. In *Organic Thin film Transistors Sensors in Organic Field-Effect Transistors*; Bao, Z., Locklin, J., Eds.; CRC, Taylor & Francis Group: Boca Raton, FL, 2007; pp 507–528; (c) Katz, H. E. Organic semiconductor-based chemical sensors In *Organic Electronic: Materials, Manufacturing and Applications*; Klauk, H., Ed.; Wiley-VCH: Weinheim, Germany, 2006; pp 411–421; (d) Wang, L.; Fine, D.; Sharma, D.; Torsi, L.; Dodabalapur, A. *Anal. Bioanal. Chem.* **2006**, 384, 310–321; (e) Torsi, L.; Dodabalapur, A. *Anal. Chem.* **2005**, 77, 380A–387A; (f) Guillaud, G.; Simon, J.; Germain, J. P. *Coord. Chem. Rev.* **1998**, 178–180, 1433–1484.
6. For selected articles see: (a) Torsi, L.; Farinola, G. M.; Marinelli, F.; Tanese, M. C.; Omar, O. H.; Valli, L.; Babudri, F.; Palmisano, F.; Zambonin, P. G.; Naso, F. *Nat. Mater.* **2008**, 7, 412–417; (b) See, K. C.; Becknell, A.; Miragliotta, J.; Katz, H. E. *Adv. Mater.* **2007**, 19, 3322–3327; (c) Huang, J.; Miragliotta, J.; Becknell, A.; Katz, H. E. *J. Am. Chem. Soc.* **2007**, 129, 9366–9376; (d) Das, A.; Dost, R.; Richardson, T.; Grell, M.; Morrison, J. J.; Turner, M. L. *Adv. Mater.* **2007**, 19, 4018–4023; (e) Torsi, L.; Dodabalapur, A.; Sabbatini, L.; Zambonin, P. G. *Sens. Actuators, B* **2000**, 67, 312–316; (f) Crone, B.; Dodabalapur, A.; Gelperin, A.; Torsi, L.; Katz, H. E.; Lovinger, A. J.; Bao, Z. *Appl. Phys. Lett.* **2001**, 78, 2229–2231; (g) Bouvet, M.; Guillaud, G.; Leroy, A.; Maillard, A.; Spirkovitch, S.; Tournilhac, F.-G. *Sens. Actuators B* **2001**, 73, 63–70; (h) Zhu, Z.-T.; Mason, J. T.; Dieckman, R.; Malliaras, G. G. *Appl. Phys. Lett.* **2002**, 81, 4643–4645; (i) Bartic, C.; Campitelli, A.; Borghs, S. *Appl. Phys. Lett.* **2003**, 82, 475–477; (j) Torsi, L.; Lovinger, A. J.; Crone, B.; Someya, T.; Dodabalapur, A.; Katz, H. E.; Gelperin, A. *J. Phys. Chem. B* **2002**, 106, 12563–12568; (k) Torsi, L.; Tanese, M. C.; Cioffi, N.; Gallazzi, M. C.; Sabbatini, L.; Zambonin, P. G.; Raos, G.; Meille, S. V.; Giangregorio, M. M. *J. Phys. Chem. B* **2003**, 107, 7589–7594; (l) Torsi, L.; Tafuri, A.; Cioffi, N.; Gallazzi, M. C.; Sassella, A.; Sabbatini, L.; Zambonin, P. G. *Sens. Actuators B* **2003**, 93, 257–262; (m) Bora, M.; Schut, D.; Baldo, M. A. *Anal. Chem.* **2007**, 79, 3298–3303.
7. (a) Afzali, A.; Breen, T. L.; Kagan, C. R. *Chem. Mater.* **2002**, 14, 1742–1746; (b) Katz, H. E.; Laquindanum, J. G.; Lovinger, A. *Chem. Mater.* **1998**, 10, 633–638; (c) Katz, H. E.; Dodabalapur, A.; Torsi, L.; Elder, D. *Chem. Mater.* **1995**, 7, 2238–2240; (d) Antolini, L.; Borsari, M.; Goldoni, F.; Iarossi, D.; Mucci, A.; Schenetti, L. *J. Chem. Soc., Perkin Trans. 1* **1999**, 3207–3212; (e) Huisman, B. H.; Valetton, J. J. P.; Nijssen, W.; Lub, J.; ten Hoeve, W. *Adv. Mater.* **2003**, 15, 2002–2005; (f) Murphy, A. R.; Fréchet, J. M. J.; Chang, P.; Lee, J.; Subramanian, V. *J. Am. Chem. Soc.* **2004**, 126, 1596–1597; (g) Yoon, M. H.; Di Benedetto, S.; Facchetti, A.; Marks, T. J. *J. Am. Chem. Soc.* **2005**, 127, 1348–1349; (h) Dell'Aquila, A.; Mastroianni, P.; Nobile, C. F.; Romanazzi, G.; Suranna, G. P.; Torsi, L.; Tanese, M. C.; Acerno, D.; Amendola, E.; Morales, P. *J. Mater. Chem.* **2006**, 16, 1183–1191; (i) Sandberg, H.; Henze, O.; Kilbinger, A. F. M.; Siringhaus, H.; Feast, W. J.; Friend, R. H. *Synth. Met.* **2003**, 137, 885–886.
8. (a) Ashizawa, M.; Kato, R.; Takanishi, Y.; Takezoe, H. *Chem. Lett.* **2007**, 36, 708–709; (b) van Breemen, A. J. J. M.; Herwig, P. T.; Chlon, C. H. T.; Sweelssen, J.; Schoor, H. F. M.; Setayesh, S.; Hardeman, W. M.; Martin, C. A.; de Leeuw, D. M.; Valetton, J. J. P.; Bastiaansen, C. W. M.; Broer, D. J.; Popa-Merticaru, A. R.; Meskers, S. C. J. *J. Am. Chem. Soc.* **2006**, 128, 2336–2345; (c) Lengyel, O.; Hardeman, W. M.; Wondergem, H. J.; de Leeuw, D. M.; van Breemen, A. J. J. M.; Resel, R. *Adv. Mater.* **2006**, 18, 896–899; (d) Funahashi, M.; Zhang, F.; Tamaoki, N.; Hanna, J.-i. *Chem. Phys. Chem.* **2008**, 9, 1465–1473; (e) Funahashi, M.; Hanna, J.-i. *Adv. Mater.* **2005**, 17, 594–598; (f) Meng, Q.; Gao, J.; Li, R.; Jiang, L.; Wang, C.; Zhao, H.; Liu, C.; Li, H.; Hu, W. *J. Mater. Chem.* **2009**, 19, 1477–1482.
9. (a) Fichou, D.; Horowitz, G. G.; Garnier, F. *Eur. Pat. Appl. EP* **1990**, 402, 269; (b) Niemi, V. M.; Knuutila, P.; Westerholm, J.-E.; Korvola, J. *Polymer* **1992**, 33, 1559–1562; (c) Abdou, M. S. A.; Lu, X.; Xie, Z. W.; Orfino, F.; Deen, M. J.; Holdcroft, S. *Chem. Mater.* **1995**, 7, 631–641; (d) Engelmann, G.; Jugelt, W.; Kossmehl, G.; Welzel, H.-P.; Tschuncky, P.; Heinze, J. *Macromolecules* **1996**, 29, 3370–3375; (e) Barbarella, G.; Zambianchi, M.; Di Toro, R.; Colonna, M., Jr.; Iarossi, D.; Goldoni, F.; Bongini, A. *J. Organomet. Chem.* **1996**, 61, 8285–8292.
10. (a) Kauffmann, T. *Angew. Chem., Int. Ed. Engl.* **1974**, 13, 291–305; (b) Kagan, J.; Arora, S. K. *Heterocycles* **1983**, 20, 1937–1940; (c) Fichou, D.; Teulade-Fichou, M.-P.; Horowitz, G.; Demanze, F. *Adv. Mater.* **1997**, 9, 75–80; (d) Bäuerle, P.; Fischer, T.; Bidlingmeier, B.; Stabel, A.; Rabe, J. P. *Angew. Chem., Int. Ed. Engl.* **1995**, 34, 303–307.
11. (a) Milstein, D.; Stille, J. K. *J. Am. Chem. Soc.* **1978**, 100, 3636–3638; (b) Stille, J. K. *Angew. Chem., Int. Ed. Engl.* **1986**, 25, 508–524.
12. Farina, V.; Krishnamurthy, V.; Scott, W. J. *The Stille Reaction*; Wiley-Interscience: New York, NY, 2000.
13. (a) Masui, K.; Ikegami, H.; Mori, A. *J. Am. Chem. Soc.* **2004**, 126, 5074–5075; (b) Takahashi, M.; Masui, K.; Sekiguchi, H.; Kobayashi, N.; Mori, A.; Funahashi, M.; Tamaoki, N. *J. Am. Chem. Soc.* **2006**, 128, 10930–10933; (c) Mori, A.; Sugie, A. *Bull. Chem. Soc. Jpn.* **2008**, 81, 548–561.
14. (a) Murphy, A. R.; Liu, J.; Luscombe, C.; Kavulak, D.; Fréchet, J. M. J.; Kline, R. J.; McGehee, M. D. *Chem. Mater.* **2005**, 17, 4892–4899; (b) Murphy, A. R.; Chang, P. C.; VanDyke, P.; Liu, J.; Fréchet, J. M. J.; Subramanian, V.; DeLongchamp, D. M.; Sambasivan, S.; Fischer, D. A.; Lin, E. K. *Chem. Mater.* **2005**, 17, 6033–6041; (c) Campione, M.; Sassella, A.; Moret, M.; Papagni, A.; Trabattini, S.; Resel, R.; Lengyel, O.; Marcon, V.; Raos, G. *J. Am. Chem. Soc.* **2006**, 128, 13378–13387; (d) Je, Y.; Nitani, M.; Ishikawa, M.; Nakayama, K.-i.; Tada, H.; Kaneda, T.; Aso, Y. *Org. Lett.* **2007**, 9, 2115–2118; (e) Zrig, S.; Koecelberghs, G.; Verbiest, T.; Andrioletti, B.; Rose, E.; Persoons, A.; Asselberghs, I.; Clays, K. *J. Org. Chem.* **2007**, 72, 5855–5858.
15. (a) Katz, H. E.; Lovinger, A. J.; Laquindanum, J. G. *Chem. Mater.* **1998**, 10, 457–459; (b) Garnier, F.; Hajlaoui, R.; El Kassmi, A.; Horowitz, G.; Laigre, L.; Porzio, W.; Armanini, M.; Provasoli, F. *Chem. Mater.* **1998**, 10, 3334–3339.
16. (a) Vidolot-Ackermann, C.; Ackermann, J.; Brisset, H.; Kawamura, K.; Yoshimoto, N.; Raynal, P.; El Kassmi, A.; Fages, F. *J. Am. Chem. Soc.* **2005**, 127, 16346–16347; (b) Vidolot-Ackermann, C.; Ackermann, J.; Kawamura, K.; Yoshimoto, N.; Brisset, H.; Raynal, P.; El Kassmi, A.; Fages, F. *Org. Electron.* **2006**, 7, 465–473; (c) Vidolot-Ackermann, C.; Brisset, H.; Zhang, J.; Ackermann, J.; Nénon, S.; Fages, F.; Marsal, P.; Tanisawa, T.; Yoshimoto, N. *J. Phys. Chem. C* **2009**, 113, 1567–1574; (d) Mauldin, C. E.; Puntambekar, K.; Murphy, A. R.; Liao, F.; Subramanian, V.; Fréchet, J. M. J.; DeLongchamp, D. M.; Fischer, D. A.; Toney, M. F. *Chem. Mater.* **2009**, 21, 1927–1938.
17. Recent literature on organic semiconductors for solution-processable OTFTs: (a) Allard, S.; Forster, M.; Souharce, B.; Thieme, H.; Scherf, U. *Angew. Chem., Int. Ed.* **2008**, 47, 4070–4098; (b) Mas-Torrent, M.; Rovira, C. *Chem. Soc. Rev.* **2008**, 37, 827–838.
18. Compounds **4TgHF** and **4TgHF₂** were isolated as pure Z isomers (¹H-NMR) whereas **8** as a 96/4 Z/E mixture.
19. The coupling constant value (³J_{HF}) between F and H at C2 in β-fluoro-α,β-unsaturated system is 25–45 Hz for the Z-isomer and 10–25 Hz for the E-isomer. See for instance: (a) Yoshida, M.; Komata, A.; Hara, S. *J. Fluorine Chem.* **2004**, 125, 527–529; (b) Peng, S.; Qing, F.-L.; Li, Y.-Q.; Hu, C.-M. *J. Org. Chem.* **2000**, 65, 694–700; (c) Xiang, J.; Jiang, W.; Gong, J.; Fuchs, P. L. *J. Am. Chem. Soc.* **1997**, 119, 4123–4129.
20. (a) Albert, P.; Cousseau, J. *J. Chem. Soc., Chem. Commun.* **1985**, 961–962; (b) Yoshida, M.; Komata, A.; Hara, S. *Tetrahedron* **2006**, 62, 8636–8645.
21. Gorgues, A.; Stephan, D.; Cousseau, J. *J. Chem. Soc., Chem. Commun.* **1989**, 1493–1494.
22. The same trend was obtained carrying out the reaction using CaCO₃ or silica gel as HF scavenger.
23. The natural abundances of ²H (0.0115%) and ¹⁷O (0.038%) are very low, therefore their contribution to the discussed peaks can be neglected.
24. Kilbinger, A. F. M.; Feast, W. J.; Cooper, H. J.; McDonnell, L. A.; Derrick, P. J.; Schenning, A. P. H. J.; Meijer, E. W. *Chem. Commun.* **2000**, 383–384.
25. In the same solvent it has been reported a λ_{max}=397 nm for the dimethyl-quaterthiophene: Miller, L. L.; Yu, Y. J. *Org. Chem.* **1995**, 60, 6813–6819 and a λ_{max}=400 nm for the dihexyl-quaterthiophene: Barbarella, G.; Favaretto, L.; Sotgiu, G.; Zambianchi, M.; Antolini, L.; Pudova, O.; Bongini, A. *J. Org. Chem.* **1998**, 63, 5497–5506.
26. Van Pham, C.; Burkhardt, A.; Shabana, R.; Cunningham, D. D., Jr.; Mark, H. B.; Zimmer, H. *Phosphorus, Sulfur Silicon Relat. Elem.* **1989**, 46, 153–168.
27. Facchetti, A.; Yoon, M.-H.; Stern, C. L.; Hutchison, G. R.; Ratner, M. A.; Marks, T. J. *J. Am. Chem. Soc.* **2004**, 126, 13480–13501.
28. (a) Melucci, M.; Zambianchi, M.; Zanelli, A.; Camaioni, N.; Gazzano, M.; Bongini, A.; Barbarella, G. *Chem. Phys. Chem.* **2007**, 8, 2621–2626 and references therein; (b) Garnier, F. *Acc. Chem. Res.* **1999**, 32, 209–215 and references therein; (c) Yassar, A.; Horowitz, G.; Valat, P.; Wintgens, V.; Hmyene, M.; Deloffre, F.; Srivastava, P.; Lang, P.; Garnier, F. *J. Phys. Chem.* **1995**, 99, 9155–9159.
29. (a) Cornil, J.; Beljonne, D.; Calbert, J. P.; Brédas, J. L. *Adv. Mater.* **2001**, 13, 1053–1059; (b) Moliton, A.; Hiorns, R. C. *Polym. Int.* **2004**, 53, 1397–1412.
30. Whitten, D. G. *Acc. Chem. Res.* **1993**, 26, 502–509.
31. Nicolas, Y.; Blanchard, P.; Roncali, J.; Allain, M.; Mercier, N.; Deman, A.-L.; Tardy, J. *Org. Lett.* **2005**, 7, 3513–3516.
32. Pommerehne, J.; Vestweber, H.; Guss, W.; Mark, R. F.; Bassler, H.; Porsch, M.; Daub, J. *Adv. Mater.* **1995**, 7, 551–554.
33. Sung, A.; Ling, M. M.; Tang, M. L.; Bao, Z.; Locklin, J. *Chem. Mater.* **2007**, 19, 2342–2351.
34. (a) Yoon, M.-H.; DiBenedetto, S. A.; Russell, M. T.; Facchetti, A.; Marks, T. J. *Chem. Mater.* **2007**, 19, 4864–4881; (b) Yoon, M. H.; Kim, C.; Facchetti, A.; Marks, T. J. *J. Am. Chem. Soc.* **2006**, 128, 12851–12869; (c) le, Y.; Umemoto, Y.; Okabe, M.; Kusunoki, T.; Nakayama, K.-i.; Pu, Y.-J.; Kido, J.; Tada, H.; Aso, Y. *Org. Lett.* **2008**, 10, 833–836.
35. Even after thermal evaporation, **4Td-g** did not show any modulation.
36. (a) Bartlett, P. A.; Otake, A. *J. Organomet. Chem.* **1995**, 60, 3107–3111; (b) Urban, J. J.; Tillman, B. G.; Cronin, W. A. *J. Phys. Chem. A* **2006**, 110, 11120–11129.
37. It is known that optimisation of the deposition conditions (temperature and/or solvent) as well as substrate pre-treatment with a suitable adhesion promoter of the organic layer onto the SiO₂ dielectric surface may improve the device performances.
38. *Purification of Laboratory Chemicals*, 5th ed.; Armarego, W. L. F.; Chai, C. L. L., Eds.; Butterworth-Heinemann: Amsterdam, 2003.
39. Bäuerle, P.; Würthner, F.; Götz, G.; Effenberger, F. *Synthesis* **1993**, 1099–1103.
40. Boas, U.; Dhanbalan, A.; Greve, D. R.; Meijer, E. W. *Synlett* **2001**, 634–635.
41. Kharash, M. S.; Seyler, R. C.; Mayo, F. R. *J. Am. Chem. Soc.* **1938**, 60, 882–884.
42. King, A. O.; Negishi, E.; Villani, F. J. J.; Silveira, A. J. *J. Organomet. Chem.* **1978**, 43, 358–360.
43. Coulson, D. R. *Inorg. Synth.* **1972**, 13, 121–124.
44. Crosby, G. A.; Demas, J. N. *J. Phys. Chem.* **1971**, 75, 991–1024.
45. Hamai, S.; Hirayama, F. *J. Phys. Chem.* **1983**, 83–89.
46. For nonaqueous electrochemistry, IUPAC recommends the use of a redox couple such as ferrocene/ferrocenium ion (Fc/Fc⁺) as an internal (or marker) standard: (a) Gritzner, G.; Küta, J. *Pure Appl. Chem.* **1984**, 56, 461–466; (b) Gritzner, G. *Pure Appl. Chem.* **1990**, 62, 1839–1858.